Negative differential resistance and quasiperiodic vortex-antivortex motion in a superconducting constriction

S. S. Ustavcshikov, M. Yu. Levichev, I. Yu. Pashenkin, and N. S. Gusev
Institute for Physics of Microstructures, Russian Academy of Sciences, 603950 Nizhny Novgorod, GSP-105, Russia

A. A. Mazilkin
Institute of Solid State Physics, Russian Academy of Sciences, 142432 Chernogolovka, Russia

D. Yu. Vodolazov*
Institute for Physics of Microstructures, Russian Academy of Sciences, 603950 Nizhny Novgorod, Russia

(Received 7 March 2024; revised 11 April 2024; accepted 8 May 2024; published 20 May 2024)

We report the observation of the negative differential resistance (NDR) in the *current*-driven regime of superconducting MoN/Cu constrictions. Our calculations in framework of time-dependent Ginzburg-Landau equation reveal that in the constriction at large current there is a channel with dynamically suppressed superconducting order parameter along which vortices and antivortices move quasiperiodically over time. As the current increases the constriction switches to the less resistive state with much faster vortices moving periodically over time (quasiphase slip-line state). Microwave radiation experiments demonstrate the presence of Shapiro steps at low voltage, where a slow, time-periodic vortex motion is expected. Conversely, Shapiro steps are absent at high voltage, where the NDR appears, indirectly confirming the quasiperiodic regime.

DOI: 10.1103/PhysRevB.109.174521

I. INTRODUCTION

In superconductors, finite resistance appears at current exceeding a critical value I_c. This occurs due to vortex motion in superconductors with size larger than the superconducting coherence length ξ or the phase slip process in small size superconducting constrictions or other types of Josephson junctions (JJ). Usually in the resistive state the voltage increases with an increase in current. In the case of vortices, it is connected to an increase of the vortex velocity, while in JJ with an increase in the oscillation frequency of the superconducting order parameter. Due to nonequilibrium effects (for example, heating [1], cooling of electrons in a moving vortex core [2], or complicated vortex dynamics [3]) the voltage-current (VI) characteristic may exhibit a region with a negative differential resistance (NDR), resulting in an S-shaped VI curve. In current-driven regime, the state with NDR is unstable and the superconductor switches to either to a low(zero)- or high-resistance state with increasing(decreasing) current, leading to a hysteretic VI characteristic.

However, there are rare phenomena when the VI curve has N shape and the NDR state is stable in the *current*-driven regime. This mainly occurs in systems where chaotic vortex motion is observed. For example, an N-shaped VI curve is realized in a superconducting film with a periodic array of artificial pinning sites and a magnetic field just above the first matching field [4–7] (where it can coexist with S-shaped VI curve [5–7]), underdamped Josephson junctions [8–10], and a superconducting constriction [11] in the presence of microwave (RF) high-power radiation. In Ref. [12] similar NDR has been predicted for asymmetric funnel arrays with moving particles/vortices where the effect originates from the rearrangement of static particles and the appearance of the so called clogging effect. An N-shaped VI curve has been also observed in Refs. [13,14], although its origin remains unclear.

In our paper, we present another superconducting system in which NDR exists in a current-driven regime. It is a superconducting strip with a wide superconducting constriction, where width $w_c \gg \xi$ and length $l_c \ll w_c$, see Fig. 1. In the constriction the current density distribution is nonuniform due to the bending of the current lines. At current $I > I_c$, the vortices enter via the left edge, where the current density is maximal, and cross the constriction. As the current increases, the number of vortices increases one by one [15–19], which is evident from the appearance of the kinks in the VI curve and oscillations in the differential resistance [see Figs. 2(a) and 2(b)]. At high current we observe N-shaped VI curve [see Figs. 2(a) and 2(b)], which is our main experimental result. Using the time-dependent Ginzburg-Landau equation coupled with the current continuity equation, we found that in this system at large current there is a channel with dynamically suppressed superconducting order parameter along which vortices and antivortices move quasiperiodically in time. As the current increases it jumps to a *less* resistive quasiphase slip-line state with faster Josephson-like vortices that move periodically in time. In this respect, it resembles results of Refs. [4–7] where the transition from chaotic to periodic vortex motion is also accompanied by a decrease in resistance. Additionally, we

*vodolazov@ipmras.ru

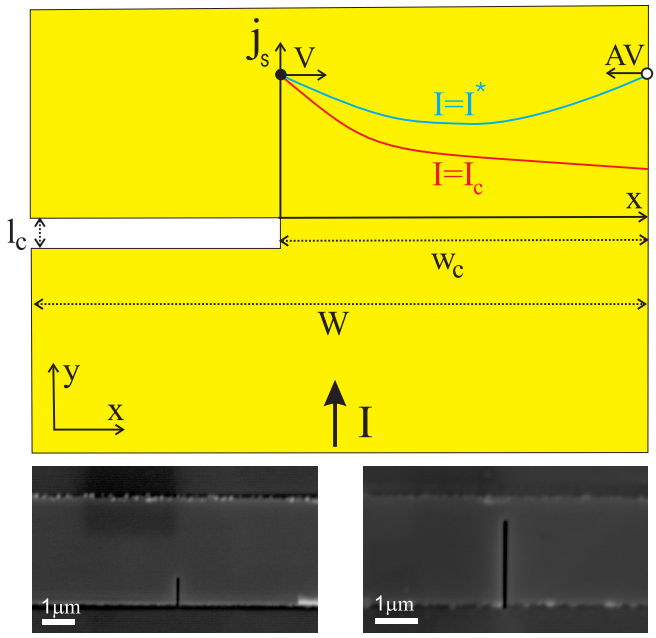

FIG. 1. Sketch of a current carrying superconducting strip with a constriction. Across the constriction there is a gradient of current density (see red and blue curves). For $I \leqslant I_c$ the gradient arises solely due to current crowding near the slit, while for $I > I_c$ the contribution from moving vortices (V) becomes important. The latter leads to a maximum of $j_s(x)$ at the right edge and the antivortex (AV) entry at $I > I^*$. Below the sketch we show micrographs of the studied MoN/Cu strips with constrictions of different widths w_c (2.5 and 0.5 μm).

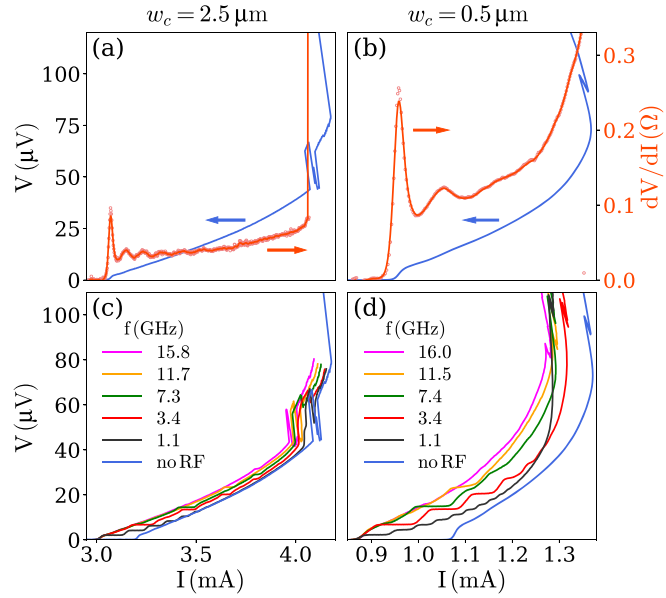

FIG. 2. [(a), (b)] Voltage-current characteristics and current-dependent differential resistance of MoN/Cu constrictions with different widths. The number of minima in the $dV/dI(I)$ dependence corresponds to the number of vortices at a given current. [(c), (d)] Voltage-current characteristics of the constrictions in the presence of microwave radiation (we adjust RF radiation power to have the same critical current at different frequencies). Measurements are done with a shunt. V(I) curves bend backward at high voltages, because in the figure I is a current flowing via superconductor, which is smaller than the total current in the presence of a shunt.

observe RF radiation-induced NDR at high electromagnetic power radiation having the same origin as in Refs. [8–11].

The structure of the paper is as follows. In Sec. II we describe our samples and experimental methods. In Sec. III we present our experimental results. In Sec. IV we show results of our modeling. In Sec. V we discuss our results and in Sec. VI make conclusions.

II. SAMPLES AND METHODS

The experiment has been carried out on MoN(40 nm)/Cu(40 nm) and MoN(40 nm)/Ni(0.5 nm)/Cu(40 nm) constrictions. MoN is a dirty superconductor with a normal state resistivity $\rho = 150\ \mu\Omega\,\text{cm}$, a critical temperature $T_c = 8.2$ K, and a coherence length $\xi(T = 0) = 4.8$ nm, while Cu is a low-resistivity metal (40-nm-thick Cu has $\rho = 2.4\ \mu\Omega\,\text{cm}$ at $T = 10$ K). The copper layer with low resistivity and high diffusion coefficient acts as a sink, allowing nonequilibrium electrons to diffuse fast away from moving vortices over a large distance (much larger than the coherence length in MoN). This enables us to suppress the influence of self-heating on vortex motion and reach a state with fast vortices before transition to the normal state. In our case, we can neglect proximity-induced superconductivity in Cu since it is strongly suppressed at $I > I_c$. This is proved by observation of the specific current dependence of the kinetic inductance $L_k(I)$ of similar MoN/Cu strips without a constriction (see Figs. 3 and 5 at zero magnetic field and discussion of $L_k(I)$ in Ref. [20]). In addition, we have samples with Ni(0.5nm) layer between Cu and MoN (Ni layer considerably suppresses proximity-induced superconductivity in Cu layer) where practically the same results are obtained.

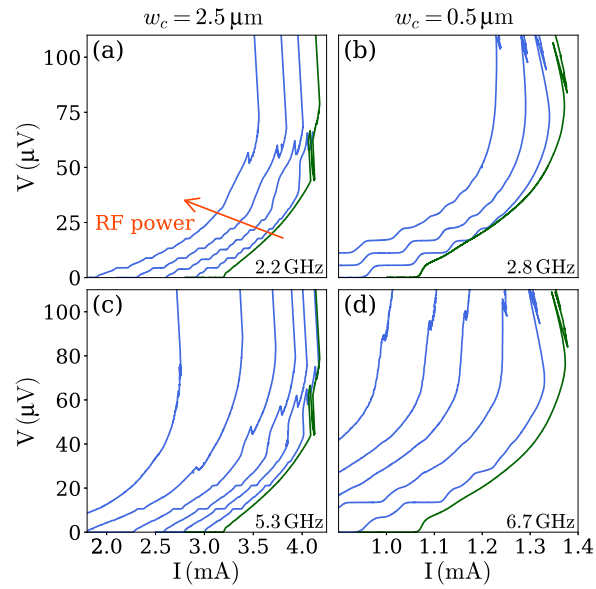

FIG. 3. Voltage-current characteristics of MoN/Cu constrictions at different power and fixed frequency of RF radiation. Measurements are done with a shunt.

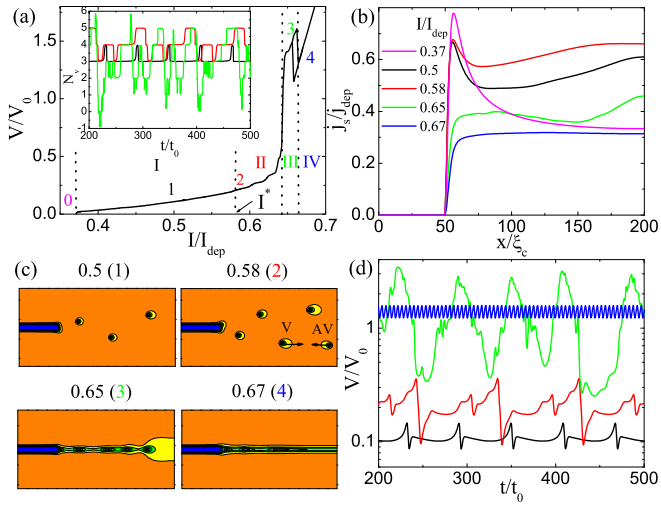

FIG. 4. (a) Calculated voltage-current characteristic of a superconducting strip with a constriction ($W = 200\xi_c$, $w_c = 150\xi_c$, $l_c = 7\xi_c$). Symbols I–IV mark the current range with different vortex dynamics. In the inset, we show the time dependence of the total vorticity in the strip $N_v = \oint \nabla\phi dl/2\pi$ at different currents (coded by color). In regime IV, only vortices are present and their number changes periodically between two and three (not shown here). (b) Time-averaged superconducting current density distribution $j_s(x)$ at the middle of the constriction at different currents, marked with symbols 0–4 in panel (a). (c) Snapshots of $|\Delta|(x, y)$ in the constriction at different currents. (d) Time-dependent voltage at different currents.

The MoN/Cu bilayers and MoN/Ni/Cu trilayers are grown at room temperature by magnetron sputtering with a base vacuum level of around 1.5×10^{-7}mbar on a silicon substrate with an native ∼2-nm-thick oxide layer. Mo is deposed in an atmosphere of a gas mixture Ar : N_2 = 10 : 1 at a pressure of 1×10^{-3} mbar and then Ni and/or Cu are deposed in an argon atmosphere at a pressure of 1×10^{-3} mbar. MoN/Cu and MoN/Ni/Cu strips with a width of 2.5 and 3.5 μm have been prepared by means of using mask-free optical lithography. We then use a Ga focused beam to make a slit and form a constriction (see Fig. 1). The slit width is about 100 nm and its length varies from 1 μm (for strips with W = 3.5 μm) to 2 μm (for strips with W = 2.5 μm). Thus, for the measurements we prepared four constrictions with a width of $w_c = 2.5$ μm (strips with W = 3.5 μm) and two constrictions with a width of $w_c = 0.5$ μm (strips with W = 2.5 μm).

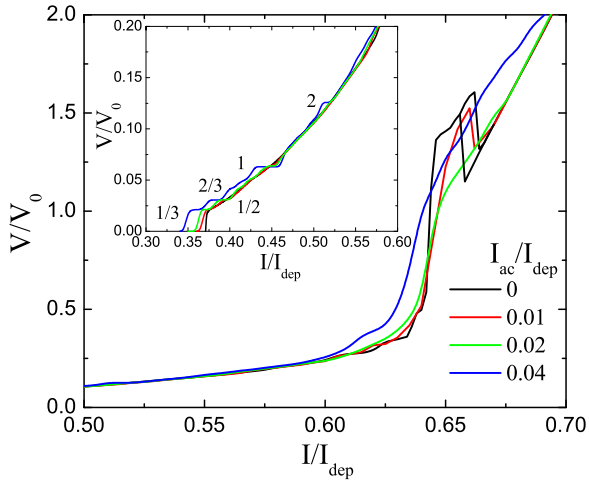

FIG. 5. Voltage-current characteristics of a superconducting strip with a constriction in the presence of AC $I_{ac}\cos(2\pi t/T_0)$ ($T_0 = 100t_0$) of different amplitude I_{ac}. In the inset, we show the low voltage part of the VI curves. The numbers indicate the positions of integer and rational Shapiro steps.

Voltage-current characteristics were measured by four-probe method. We used a 0.8 Ω shunt connected in parallel with the superconducting strip to prevent the strip from switching to a high-resistance state due to environment noise. This allowed us to reach NDR region of the VI curve in the absence of microwave radiation. The shunt was placed on the distance less than 1 cm from the samples. We checked that without the shunt we obtained similar results (the results without the shunt are presented in Appendix B). All measurements were carried out at 4.2 K; the critical temperature of the hybrids was about 7.8 K.

To check the presence of periodic vortex motion we applied microwave radiation in the frequency range $f = 0.5 - 20$ GHz. The radiation was generated by a whip antenna without impedance matching (for more details, see Ref. [11]).

III. EXPERIMENTAL RESULTS

In Figs. 2(a) and 2(b) we show typical VI curves for constrictions of various widths. Above the critical current, oscillations in differential resistance are clearly visible, which are fingerprints of a change in the vortex number [16–19]. We have at least 7 or 2 vortices in the constriction (depending on its width), which corresponds to the number of minima in $dV/dI(I)$ dependence. In the voltage range where oscillations exist, Shapiro RF-induced steps are observed [see Figs. 2(c) and 2(d)], validating the time periodicity of the vortex motion. At high voltages, there is a region of negative differential resistance on the VI curve. At voltages slightly below this, dV/dI oscillations are not visible, and Shapiro steps are absent. VI characteristics are reversible when measured without a shunt, unless the constriction jumps to a more resistive state with a resistance of about 1 Ω (with a shunt they are reversible at any current).

In Fig. 3 we show evolution of the VI curves with increasing RF power. Shapiro steps do not appear near and below NDR region, and the NDR amplitude decreases. At a fixed RF power, the latter effect is more pronounced at higher frequencies.

IV. QUASIPERIODIC VORTEX-ANTIVORTEX MOTION

To study the origin of the found NDR, we modeled vortex dynamics and calculated VI characteristic of superconducting strip with a constriction using the ordinary time-dependent Ginzburg-Landau equation (equations and details of the model are presented in Appendix A). In Fig. 4 we show our results, where the voltage is normalized in units of $V_0 = k_B T_c/|e|$, the current is in units of strip depairing current

without constriction I_{dep}, the time is in units of $t_0 = \hbar/k_B T_c$, and the distance is in units of $\xi_c = \sqrt{\hbar D/k_B T_c}$ (D is the diffusion coefficient). At $I > I_c = 0.37 I_{dep}$, the vortices enter the strip at the place where the current density is maximal [near the tip of the slit, see Figs. 1 and 4(b)] and move across the constriction. With increasing current their number increases one by one and it leads to kinks in VI curve [15–19] and the appearance of a vortex jet due to vortex repulsion [17–19,21], see Fig. 4(c) at $I = 0.5 I_{dep}$. This regime is marked with the symbol I in Fig. 4(a).

The vortices in the constriction change the current distribution—the current density from vortices and the transport current are summed up at the right edge of the constriction [see Fig. 4(b)]. As a result for $I \geqslant I^* = 0.58 I_{dep}$, when the current density at the right edge reaches depairing value, the antivortices enter the strip and annihilate with the vortices inside the constriction (see movie at $I = 0.58 I_{dep}$ within the Supplemental Material, SM [22])—we marked this regime with the symbol II in Fig. 4(a). This complicates the vortex-antivortex dynamics, and the period $V(t)$ *increases*, as one can see in Fig. 4(d). This periodic regime is replaced by a "chaotic" V-AV motion (without any visible period or quasiperiod) in a narrow current interval $(0.63 - 0.642) I_{dep}$, where the vortex jet still exists. It is interesting to note that in the "chaotic" regime, unusual dynamics is observed when V-AV do not annihilate and pass through each other (see movie at $I = 0.63 I_{dep}$ within the SM [22]).

For $I \geqslant 0.644 I_{dep}$, a sharp increase in voltage occurs due to shrinking of the vortex jet and the appearance of an area with a dynamically suppressed order parameter [see Fig. 4(c)] along which vortices and antivortices move faster than in the vortex jet regime [regime III in Fig. 4(a)]. This vortex-line state arises due to finite relaxation time of Δ (τ_Δ)—at relatively large vortex velocity and number of vortices the superconducting order parameter does not have time to recover after the vortex passage, and a channel appears with suppressed $|\Delta|$ along which vortices and antivortices move. Physically similar state has been studied previously in several papers (see for example [23–25]), experimentally visualized [26–28] and exists in our system too, but in regime IV. In that state there are Josephson-like vortices of only one sign (except a symmetrical superconductor in zero magnetic field [23,24]), which move periodically in time and physically it resembles the phase slip line in a wide superconducting strip [23,29,30]. The vortex (phase slip)-line state should be distinguished from the vortex river state, which may appear in intrinsically or artificially inhomogeneous superconductors where there are easy paths for Abrikosov vortex motion, as for example the rows of holes in Refs. [4–7].

In regime III, a quasiperiodic V-AV motion is observed, leading to a quasiperiodic $V(t)$ [see Fig. 4(d)]. Total vorticity at some moments of time becomes equal to zero or even negative [see inset in Fig. 4(a)], which means that the number of vortices is equal to or less than the number of antivortices. The V-AV annihilate or pass through each other, and then new vortices and antivortices quickly enter the constriction, and this process repeats (see movie at $I = 0.65 I_{dep}$ within the SM [22]). Note that the temporary nucleus of the V-AV lines appear in the "chaotic" part of regime II in different branches of the vortex jet (see movie at $I = 0.638 I_{dep}$ within the SM [22]), and only at higher current V-AV line becomes a stable state.

The transition from regime III to regime IV is abrupt, and it is accompanied by a *decrease* in voltage. In regime IV maximal number of vortices is 3, which is significantly less than in regime III, where the number of vortices and antivortices can reach 7, but they move much faster providing not a very large voltage drop. The reverse transition is also sharp and occurs at a slightly lower current, leading to a hysteretic VI curve. With the current step used ($0.002 I_{dep}$), we found no hysteresis during transition between a vortex line with quasiperiodic V-AV motion (regime III) and a vortex jet with periodic/"chaotic" V-AV motion (regime II).

Application of AC induces integer and rational Shapiro steps at low voltages and destroys the NDR (see Fig. 5). As in the absence of AC the number of vortices increases one by one with increasing DC, which form a vortex jet and antivortices appear at I^* depending on I_{ac}. A sharp increase in voltage occurs due to the transition from the "chaotic" V-AV jet to the quasiperiodic V-AV line state, but the next transition to periodic vortex-line state with smaller number of vortices is reversible and without NDR already at $I_{ac} = 0.02 I_{dep}$ [where time periodic voltage $V(t)$ is the sum of two signals with a period of AC T_0 and a significantly shorter period associated with the passage of fast vortices through the constriction].

V. DISCUSSION

The nonuniform current distribution in the constriction is a necessary condition for the occurrence of quasiperiodic vortex-antivortex motion and NDR in the superconducting constriction. Indeed, in the case of $j(x) = \text{const}$, even in a wide strip with $W \gg \xi$ vortex motion is not realized at $I > I_c = I_{dep}$ and superconductor jumps either to a normal or to a resistive state with a phase slip line. Only in the presence of j_s gradient a resistive state with vortex motion can exist at zero magnetic field. At high currents, the number of vortices and their velocity become large enough to ensure $\tau_{V-V} < \tau_\Delta$, where τ_{V-V} is the time required for the vortex to traverse the intervortex distance. This leads to the deformation of the vortex cores (Δ does not have time to recover after vortex passage) and to the formation of a channel with suppressed Δ (regimes III, IV). In our system, a current density gradient exists across the constriction [see Fig. 4(b)], and both the vortex velocity and τ_Δ depend on the local current density j_s (where higher j_s results in smaller τ_Δ [31,32]). However, j_s is influenced by the vortex distribution within the constriction. Taken together, this considerably complicates the V-AV dynamics and leads to their quasiperiodic motion. In regime IV, j_s remains constant, and since the vortices are Josephson rather than Abrikosov vortices, they make a small contribution to j_s (i.e., j_s exhibits weak dependence on the number of vortices and their distribution within the channel), resulting in periodic vortex motion over time. But even with nonuniform $j_s(x)$, as our calculations reveal (see Appendix A) the quasiperiodic regime and NDR are realized only for certain parameters in the time-dependent Ginzburg-Landau model, which control τ_Δ.

In contrast, the oscillations of the differential resistance and the vortex jet are more robust phenomena and exist even in the London model [15,17,21]. The same is probably true for the antivortex entry at $I > I^*$, since a similar effect has been predicted for a wide superconducting strip where the current density is nonuniform due to the Meissner effect [23,33]. In that system, due to the symmetry, local maximum of $j_s(x)$ is located in the center of the strip and at a certain current (similar to our I^*) the vortex-antivortex motion is replaced by an array of phase slip lines [23]. This prediction has been confirmed by numerical modeling in the framework of the generalized time-dependent Ginzburg-Landau equation [24]. Here we found that the situation may be more complex—there is a vortex line with quasiperiodic relatively slow V-AV motion [regime III in Fig. 4(a)] with a resistance larger than that of the line state with fast vortices [regime IV in Fig. 4(a)]. In addition, there is regime with periodic/chaotic slow vortex-antivortex motion [regime II in Fig. 4(a)], which has not been discussed previously.

While our simulations qualitatively explain the presence of NDR in MoN/Cu constriction, there are quantitative differences between experiment and theory. Firstly, in the experiment VI curve is reversible, while in theory hysteresis is observed when the constriction switches between regimes III and IV. This discrepancy can be explained by environment noise, which may destroy this small hysteresis.

Secondly, in theory the NDR disappears at a small amplitude of the AC, when the critical current changes insignificantly, while in experiment it persists up to high RF power with a large shift of I_c. We speculate that the Cu layer may be responsible for this effect. Indeed, the electric field of RF radiation accelerate superconducting electrons and induces RF superconducting current in the superconductor. The RF supercurrent reduces critical current of the constriction, as observed in the experiment. In the resistive state, due to large difference in ρ between MoN and Cu layers, part of the normal current must flow through the Cu layer (this effect reaches its maximal value with the appearance of a the vortex river). The RF supercurrent is partially converted to the normal current in the constriction when it is in a resistive state, and part of this current flows through the Cu layer. This leads to a decrease in the amplitude of RF current in MoN. In other words, in the resistive state we expect a smaller amplitude of the RF current flowing in MoN than in the superconducting state, and the difference increases with increase in voltage. Actually, the Cu layer acts as a shunt when the MoN layer is in the resistive state, and part of the current flows through the copper. In simulations we cannot take this into account, since it would require using 3D model, which is a rather time consuming task.

VI. CONCLUSIONS

Our main experimental result is the observation of negative differential resistance (NDR) in the current-driven regime of superconducting MoN/Cu constrictions. We attribute this observation to the presence of a copper layer, which serves as a radiator cooling nonequilibrium electrons generated by vortex motion within the superconducting constriction. In the presence of microwave radiation, Shapiro steps appear at low voltages. Together with the current oscillations in differential resistance, this proves the existence of periodic vortex motion. Conversely, at high voltages, where NDR appears, Shapiro steps are not observed.

Our calculations, based on the numerical solution of the time-dependent Ginzburg-Landau equation, demonstrate the presence of a channel within the constriction at high currents, wherein the superconducting order parameter is dynamically suppressed. Within this channel, vortices and antivortices exhibit quasiperiodic motion over time. This state demonstrates higher resistance compared to the state at higher currents, where vortices move periodically at much faster velocity. We relate the discovered quasiperiodicity to the dependence of relaxation time of the superconducting order parameter on the local current density, which in turn depends on the vortex distribution within the constriction. Notably, in simulations, Shapiro steps are not observed at high voltages, where periodic vortex motion is absent. This result corroborates our experimental findings.

ACKNOWLEDGMENTS

Authors acknowledge the support by Russian Science Foundation, Project No. 23-22-00203 and the facility centers at the Institute of Solid State Physics of Russian Academy of Sciences in sample treatment.

APPENDIX A: MODEL

We calculate the voltage-current characteristic of a superconducting strip with a constriction using the ordinary time-dependent Ginzburg-Landau equation for the superconducting order parameter $\Delta = |\Delta| \exp(i\phi)$,

$$u\frac{\pi\hbar}{8k_BT_c}\left(\frac{\partial}{\partial t}+\frac{2ie\varphi}{\hbar}\right)\Delta = \frac{\pi}{8}\xi_c^2\left(\nabla - i\frac{2e}{\hbar c}A\right)^2\Delta + \left(1-\frac{T}{T_c}-\frac{|\Delta|^2}{\Delta_{GL}^2}\right)\Delta \quad \text{(A1)}$$

coupled with current continuity equation

$$div\, j = div\,(j_s + j_n) = div\left(-\frac{\sigma_n}{e}\frac{\pi|\Delta|^2 q_s}{4k_BT_c} - \sigma_n\nabla\varphi\right) = 0 \quad \text{(A2)}$$

In Eqs. (A1) and (A2) T_c is the critical temperature, D is the diffusion coefficient, $\sigma_n = 2e^2DN_0$ is the conductivity, N_0 is the density of states, $q_s = (\nabla\phi - 2eA/\hbar c)$ is the momentum of Cooper pairs (in our case $A = 0$, since we do not have a magnetic field), $\xi_c^2 = \hbar D/k_BT_c$, $\Delta_{GL} = 3.06k_BT_c$. The phenomenological parameter u controls the time variation of $|\Delta|$: $\tau_{|\Delta|} \sim u$. The value of the parameter u may be different in different materials, for example due to variation of inelastic electron-phonon relaxation time τ_{ep} because $\tau_{|\Delta|} \sim \tau_{ep}$ as follows from the generalized TDGL model [34].

We solve numerically the Eqs. (A1) and (A2) only in the superconductor, because we assume that in the N layer the proximity-induced superconductivity is suppressed by the current. We neglect the heating of electrons due to dissipation and their cooling due to time-dependent $|\Delta|$ {the latter effect may lead to a long relaxation time of $|\Delta|$ [31,32], instability of the vortex motion [2] and different form of Eqs. (A1)

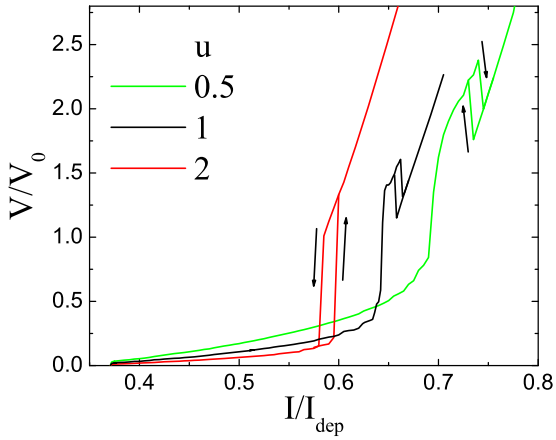

FIG. 6. Calculated VI curves of a superconducting strip with a constriction at different values of the parameter u in Eq. (A1).

and (A2) [34]}. We assume that nonequilibrium electrons created by moving vortices, diffuse away from the constriction through the N layer, which has a large diffusion coefficient and a zero-energy gap. Therefore, we have an almost equilibrium situation in the superconductor and expect a small value of the parameter u leading to a small $\tau_{|\Delta|}$.

In the calculations we choose $W = 200\xi_c$, $l_c = 7\xi_c$, $w_c = 150\xi_c$, length of the strip $L = 240\xi_c$, $T/T_c = 0.8$. To "inject" current into the strip we use the normal metal-superconductor boundary conditions in the y direction, $\Delta(y = \pm L/2) = 0$, $-\sigma_n \nabla\varphi|_{\pm L/2} = I/Wd$ and isolator-superconductor boundary conditions in the x direction, $\partial\Delta/\partial x|_{\pm W/2} = 0$, $\nabla\varphi|_{\pm W/2} = 0$. The slit is modelled as a region with a critical temperature 2.5 times smaller than in the over part of the superconductor. Most of the calculations (in particular, results in Figs. 4 and 5) have been carried out at $u = 1$.

In Fig. 6 we show the impact of u on the VI curves. As u increases, the vortices move slower because of the larger $\tau_{|\Delta|}$ and the slope of the VI curve decreases in the slow vortex motion mode, corresponding to regimes I–II in Fig. 4(a). At the same time, other properties [kinks, vortex jet, antivortex entry at $I > I^*(u)$] remain qualitatively the same. The river state with quasiperiodic V-AV dynamics is not realized at $u = 2$ and system jumps from regime II to regime IV and vice versa, leading to the hysteretic VI characteristic without N-like area. The hysteresis here is not associated with heating (we do not take it into account), but originates from the competition between the time variation of $|\Delta|$ and $\nabla\phi$, as in superconducting microbridge with $l_c \gg w_c \sim \xi$ [35]. For $u = 1/2$, the range of the currents where quasiperiodic V-AV motion exists is larger than for $u = 1$. Our findings indicate the importance of intrinsic time τ_Δ on emergence of quasiperiodic V-AV motion and NDR in a superconducting constriction.

APPENDIX B: EXPERIMENT WITHOUT SHUNT

In Fig. 7(a) we show the results for the MoN/Cu constriction with $w_c = 0.5$ nm (the same sample as in Figs. 2 and 3) without a shunt. The VI curve is the same as with a shunt, except that at lower current there is a jump to a more resistive

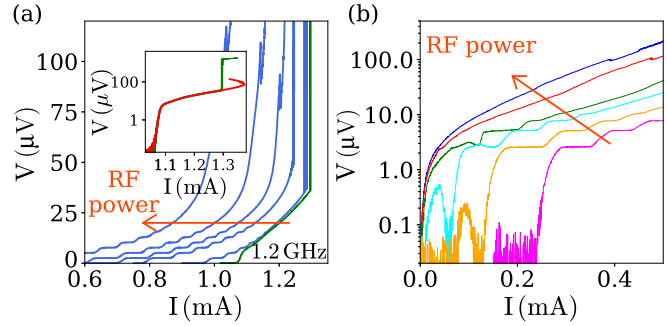

FIG. 7. (a) Voltage-current characteristics of a constriction with $w_c = 0.5$ μm without a shunt in the presence of RF radiation. In the inset of panel (a), we compare the VI curves with (red) and without (green) shunt in the absence of microwaves. In panel (b) we show another type of NDR, which appears at high RF radiation power.

state, see inset in Fig. 2(a). Note that the evolution of the VI curves with increasing RF radiation power is the same as when using a shunt.

At high RF radiation power (when $I_c \to 0$), another type of NDR appears at low currents and voltages, similar to that observed in Refs. [8–11], see Fig. 7(b). Note the quantitative difference between the NDR at zero/low and high RF radiation power.

APPENDIX C: SAMPLES WITH NI LAYER

In Fig. 8 we present the VI curves of the MoN(40)/Ni(0.5)/Cu(40) constriction (we have two samples with W = 3.5 μm and $w_c = 2.5$ μm with very similar properties). One can see an N-like region and oscillations

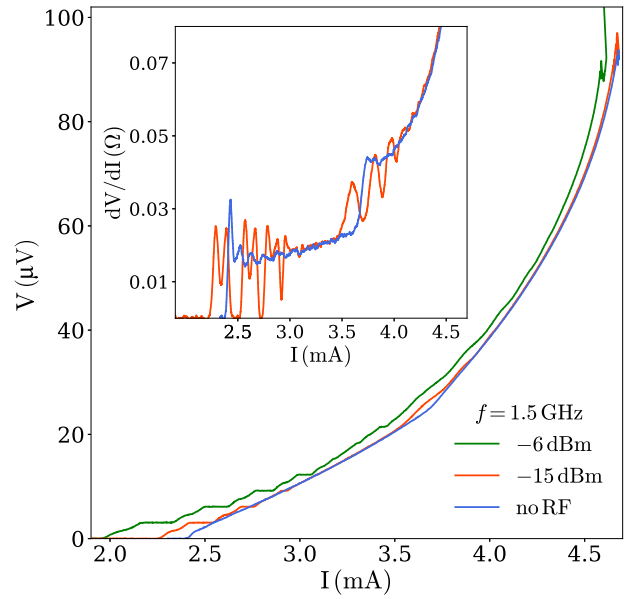

FIG. 8. Voltage-current characteristics of MoN/Ni/Cu constriction with $w_c = 2.5$ μm. In the inset we show dependence of the differential resistance on the current. In this sample we observe sharp increase of dV/dI at $I \sim 3.7$ mA, which we relate with the vortex entry via intrinsic defect away from a constriction. It is proved by response on RF radiation, which is typical for two connected in series Josephson junctions with different critical currents.

of differential resistance at low voltages, corresponding to vortex number change. This result shows that the effect of the proximity-induced superconductivity in the Cu layer is negligible. Compared to the MoN/Cu samples, we observe a large change in dV/dI at current a $I_d \sim 3.7$ mA, which we relate to vortex entry through an intrinsic edge defect far away from the constriction. An experiment with RF radiation proves this—there are radiation-induced features in differential resistance both near I_c and I_d (see inset in Fig. 8), which resembles the situation with Shapiro steps for two connected in series Josephson junctions with different critical currents I_c and I_d. While at $I < I_d$ Shapiro steps appear at voltages $V_n = nf\Phi_0/2$ (n is an integer number), at $I > I_d$ they are smeared and located at different voltages (their position depends on the power of RF radiation) and I_d decreases, similar to I_c.

[1] A. V. Gurevich and R. G. Mints, Self-heating in normal metals and superconductors, Rev. Mod. Phys. **59**, 941 (1987).

[2] A. I. Larkin and Y. N. Ovchinnikov, Nonlinear conductivity of superconductors in the mixed state, Zh. Eksp. Teor. Fiz. **68**, 1915 (1975) [Sov. Phys. JETP **41**, 960 (1975)].

[3] C. Reichhardt, C. J. Olson, and F. Nori, Nonequilibrium dynamical phases and plastic flow of driven vortex lattices in superconductors with periodic arrays of pinning sites, Phys. Rev. B **58**, 6534 (1998).

[4] C. Reichhardt, C. J. Olson, and F. Nori, Dynamic phases of vortices in superconductors with periodic pinning, Phys. Rev. Lett. **78**, 2648 (1997).

[5] V. R. Misko, S. Savel'ev, A. L. Rakhmanov, and F. Nori, Nonuniform self-organized dynamical states in superconductors with periodic pinning, Phys. Rev. Lett. **96**, 127004 (2006).

[6] V. R. Misko, S. Savel'ev, A. L. Rakhmanov, and F. Nori, Negative differential resistivity in superconductors with periodic arrays of pinning sites, Phys. Rev. B **75**, 024509 (2007).

[7] J. Gutierrez, A. V. Silhanek, J. Van de Vondel, W. Gillijns, and V. V. Moshchalkov, Transition from turbulent to nearly laminar vortex flow in superconductors with periodic pinning, Phys. Rev. B **80**, 140514(R) (2009).

[8] N. F. Pedersen, O. H. Soerensen, B. Dueholm, and J. Mygind, Half-harmonic parametric oscillations in Josephson junctions, J. Low Temp. Phys. **38**, 1 (1980).

[9] C. Noeldeke, R. Gross, M. Bauer, G. Reiner, and H. Seifert, Experimental survey of chaos in the Josephson effect, J. Low Temp. Phys. **64**, 235 (1986).

[10] J. Nagel, D. Speer, T. Gaber, A. Sterck, R. Eichhorn, P. Reimann, K. Ilin, M. Siegel, D. Koelle, and R. Kleiner, Observation of negative absolute resistance in a Josephson junction, Phys. Rev. Lett. **100**, 217001 (2008).

[11] S. S. Ustavschikov, M. Yu. Levichev, I. Yu. Pashen'kin, N. S. Gusev, S. A. Gusev, and D. Yu. Vodolazov, Negative differential resistance and Shapiro steps in a superconducting MoN strip with a cut, JETP Lett. **115**, 626 (2022).

[12] C. J. O. Reichhardt and C. Reichhardt, Clogging and transport of driven particles in asymmetric funnel arrays, J. Phys.: Condens. Matter **30**, 244005 (2018).

[13] R. P. Huebener and D. E. Gallus, Negative differential resistivity in superconductors at high current densities, Appl. Phys. Lett. **22**, 597 (1973).

[14] O. V. Dobrovolskiy, M. Huth, V. A. Shklovskij, and R. V. Vovk, Mobile fluxons as coherent probes of periodic pinning in superconductors, Sci. Rep. **7**, 13740 (2017).

[15] L. G. Aslamazov and A. I. Larkin, Josephson effect in wide superconducting bridges, Zh. Eksp. Teor. Fiz. **68**, 766 (1975) [Sov. Phys. JETP **41**, 381 (1975)].

[16] M. J. M. E. de Nivelle, W. A. M. Aarnink, M. V. Pedyash, E. M. C. M. Reuvekamp, D. Terpstra, M. A. J. Verhoeven, G. J. Gerritsma, and H. Rogalla, Vortex motion and Josephson effect in superconducting bridges in (001) and (105) oriented $YBa_2Cu_30_{7-\delta}$ thin films, IEEE Trans. Appl. Supercond. **3**, 2512 (1993).

[17] M. V. Pedyash, G. J. Gerritsma, D. H. A. Blank, and H. Rogalla, Coherent vortex motion in superconducting nanobridges based on YBaCuO thin films, IEEE Trans. Appl. Supercond. **5**, 1387 (1995).

[18] V. M. Bevz, M. Yu. Mikhailov, B. Budinska, S. Lamb-Camarena, S. O. Shpilinska, A. V. Chumak, M. Urbánek, M. Arndt, W. Lang, and O. V. Dobrovolskiy, Vortex counting and velocimetry for slitted superconducting thin strips, Phys. Rev. Appl. **19**, 034098 (2023).

[19] S. S. Ustavshchikov, M. Yu. Levichev, I. Yu. Pashen'kin, N. S. Gusev, S. A. Gusev, and D. Yu. Vodolazov, Vortex dynamics in superconducting MoN strip with a side cut, J. Exp. Theor. Phys. **137**, 372 (2023).

[20] M. Yu. Levichev, I. Yu. Pashenkin, N. S. Gusev, and D. Yu. Vodolazov, Finite momentum superconductivity in superconducting hybrids: Orbital mechanism, Phys. Rev. B **108**, 094517 (2023).

[21] A. I. Bezuglyj, V. A. Shklovskij, B. Budinska, B. Aichner, V. M. Bevz, M. Yu. Mikhailov, D. Yu. Vodolazov, W. Lang, and O. V. Dobrovolskiy, Vortex jets generated by edge defects in current-carrying superconductor thin strips, Phys. Rev. B **105**, 214507 (2022).

[22] See Supplemental Material at http://link.aps.org/supplemental/10.1103/PhysRevB.109.174521 for the movies, which illustrate vortex and vortex-antivortex dynamics at different currents.

[23] S. V. Lempitskii, Phase slippage lines in wide superconducting films, Zh. Eksp. Teor. Fiz. **90**, 793 (1986) [Sov. Phys. JETP **63**, 462 (1986)].

[24] D. Y. Vodolazov and F. M. Peeters, Rearrangement of the vortex lattice due to instabilities of vortex flow, Phys. Rev. B **76**, 014521 (2007).

[25] G. Grimaldi, A. Leo, P. Sabatino, G. Carapella, A. Nigro, S. Pace, V. V. Moshchalkov, and A. V. Silhanek, Speed limit to the Abrikosov lattice in mesoscopic superconductors, Phys. Rev. B **92**, 024513 (2015).

[26] A. G. Sivakov, A. M. Glukhov, A. N. Omelyanchouk, Y. Koval, P. Muller, and A. V. Ustinov, Josephson behavior of

phase-slip lines in wide superconducting strips, Phys. Rev. Lett. **91**, 267001 (2003).

[27] A. V. Silhanek, M. V. Milosevic, R. B. G. Kramer, G. R. Berdiyorov, J. Van de Vondel, R. F. Luccas, T. Puig, F. M. Peeters, and V. V. Moshchalkov, Formation of stripelike flux patterns obtained by freezing kinematic vortices in a superconducting Pb film, Phys. Rev. Lett. **104**, 017001 (2010).

[28] L. Embon, Y. Anahory, Z. L. Jelic, E. O. Lachman, Y. Myasoedov, M. E. Huber, G. P. Mikitik, A. V. Silhanek, M. V. Milosevic, A. Gurevich, and E. Zeldov, Imaging of super-fast dynamics and flux instabilities of superconducting vortices, Nat. Commun. **8**, 85 (2017).

[29] S. G. Zybtsev, I. G. Gorlova, and V. Ya. Pokrovski, Dynamic mixed state in micron-size bridges based on $Bi_2Sr_2CaCu_2O_x$ whiskers, JETP Lett. **74**, 168 (2001).

[30] V. M. Dmitriev, I. V. Zolochevskii, T. V. Salenkova, and E. V. Khristenko, Resistive current state of a wide superconducting film, Low Temp. Phys. **31**, 127 (2005).

[31] J. A. Pals and J. Wolter, Measurement of the order-parameter relaxation in superconducting Al-strips, Phys. Lett. A **70**, 150 (1979).

[32] M. Tinkham, in *Nonequilibrium, Superconductivity, Phonons, and Kapitza Boundaries*, in *Proceedings of NATO Advanced Study Institutes*, edited by K. E. Gray (Springer, New York, 1981), p. 231.

[33] L. G. Aslamazov and S. V. Lempitskii, Resistive state in broad superconducting films, Zh. Eksp. Teor. Fiz. **84**, 2216 (1983) [Sov. Phys. JETP **57**, 1291 (1983)].

[34] R. J. Watts-Tobin, Y. Krahenbuhl, and L. Kramer, Nonequilibrium theory of dirty, current-carrying superconductors: phase-slip oscillators in narrow filaments near T_c, J. Low Temp. Phys. **42**, 459 (1981).

[35] D. Y. Vodolazov and F. M. Peeters, Origin of the hysteresis of the current-voltage characteristics of superconducting microbridges near the critical temperature, Phys. Rev. B **84**, 094511 (2011).